NANO LETTERS

2007
Vol. 7, No. 7
2142−2145

Scrolled Sheet Precursor Route to Niobium and Tantalum Oxide Nanotubes

Yoji Kobayashi,[†] Hideo Hata,[†] Magda Salama,[‡] and Thomas E. Mallouk*,[†]

Department of Chemistry, The Pennsylvania State University, University Park, Pennsylvania 16802, and 109 Materials Research Laboratory, Materials Research Institute, The Pennsylvania State University, University Park, Pennsylvania 16802

Received April 8, 2007; Revised Manuscript Received May 25, 2007

ABSTRACT

The nanoscroll-to-nanotube thermal transformation was studied for $H_4Nb_6O_{17}\cdot 4.4H_2O$ scrolls, prepared by exfoliation of $K_4Nb_6O_{17}$. Thermal dehydration of the scrolls produces Nb_2O_5 nanotubes at 400−450 °C. The nontopochemical transformation results in polycrystalline nanotubes; however, significant texturing with respect to the tube axis is observed. Substituting Ta for Nb in the precursor compound led to a lower yield of scrolls, most likely because there is less built-in lattice strain to drive scrolling of the unilamellar colloidal sheets.

Layered materials that can be exfoliated chemically to make unilamellar colloids possess the interesting possibility of restacking by scrolling into tubular morphologies. This has already been demonstrated in oxides such as $K_4Nb_6O_{17}$[1,2] and V_2O_5[3,4] and with non-oxide layered materials such as carbon[5] and the layered chalcogenides.[6] Other studies of nanotubes using hydrothermal or template methods exist.[7−11] However, few studies exist on the transformation of the scroll structures, which are still layered in nature, to closed nanotubes. To date, most of the relevant studies concern titania nanotubes made from a scrolled layered alkali or protonated titanate.[12−18] However, this process remains limited in scope mainly to the formation of TiO_2 nanotubes and to a single example with MnO_2 nanotubes.[19] Despite this, there exist many other layered oxides that readily exfoliate into unilamellar colloids. Among these, many are known to undergo topochemical reactions in the solid state.[20] Can these be scrolled and undergo further reaction to form nanotubes?

Several papers have been published on the spontaneous scrolling of $K_{1-x}H_xNb_6O_{17}$ upon exfoliation by aqueous tetra-(*n*-butyl)ammonium hydroxide (TBAOH).[1] Because this is one of the few oxide materials that are known to scroll readily, we chose it to study the transformation into Nb_2O_5 nanotubes. Unfortunately, this transformation cannot happen topochemically, and the resulting nanotubes are therefore not single crystalline. However, we find that after thermal conversion, the nanotubular morphology is still preserved with some texturing despite the extensive rearrangement of atoms. This is an encouraging result as we attempt to identify other materials that can be scrolled (perhaps using methods recently developed by Ma et al.[21]) and topochemically transformed into nanotubes.

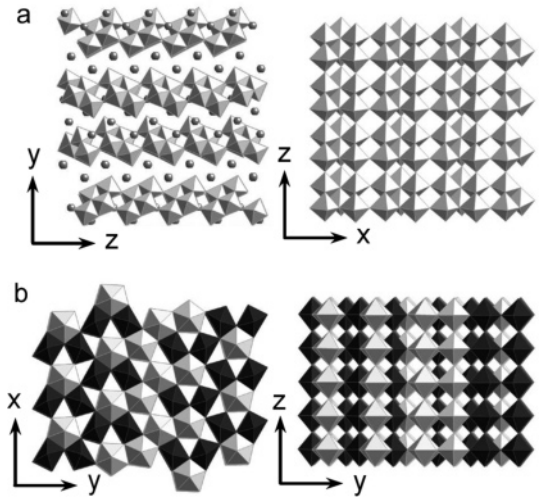

Figure 1. Crystal structure of **(a)** $K_4Nb_6O_{17}$ and **(b)** T−Nb_2O_5.

The layered structure of $K_4Nb_6O_{17}$ is shown in Figure 1a. Each layer is composed of edge-sharing NbO_6 octahedra. Close examination reveals that, for each layer, the top and bottom faces are different from each other, as exhibited by the different interlayer cation arrangements.[22] It is thought that this asymmetry in the faces of the sheets leads to spontaneous scrolling when the proton-exchanged compound $K_xH_{1-x}Nb_6O17$ is exposed to aqueous TBAOH.[1] Figure 2a shows an image of $TBA_xH_{1-x}Nb_6O_{17}$ scrolls obtained after exfoliation and scrolling in aqueous TBAOH. As previous authors have noted, scrolling occurs in high yield, with diameters of about 30 nm and lengths of a few hundred nanometers. On the basis of statistical TEM measurements, Saupe et al. and Du et al. concluded that the scrolls are

* Corresponding author. E-mail: tom@chem.psu.edu.
[†] Department of Chemistry.
[‡] Materials Research Institute.

10.1021/nl0708260 CCC: $37.00
Published on Web 06/21/2007

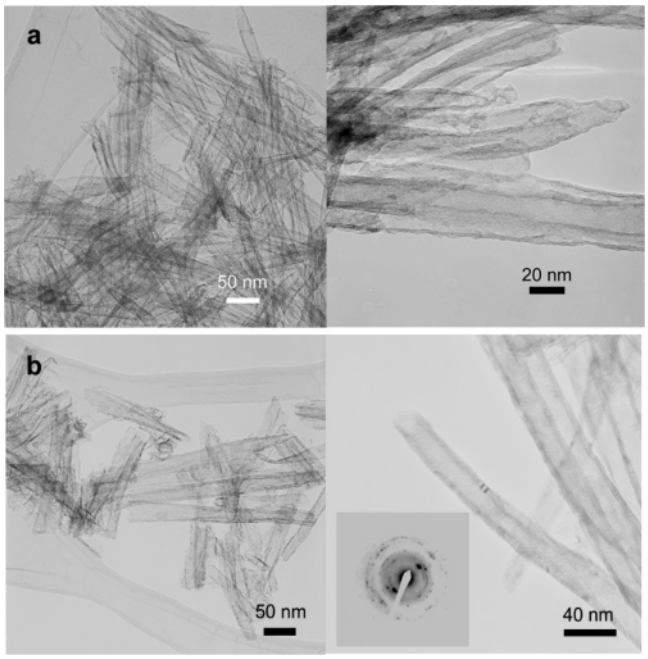

Figure 2. TEM images of **(a)** $H_4Nb_6O_{17}{\cdot}nH_2O$ scrolls, after isolation as a powder and of **(b)** Nb_2O_5 nanotubes obtained by treatment at 400 °C, 30 min (left) and 425 °C, 3 h (right).

formed by exfoliated layers scrolling chiefly in the [100] direction, with the *z* axis of the original crystal structure as the tube axis.[1,23] There was a small portion of unscrolled sheets also present in some batches. Energy dispersive X-ray spectroscopy (EDS) showed that no detectable amount of potassium remained in the scrolls.

X-ray diffraction (XRD) patterns for the nanoscrolls isolated as powders are shown in the upper portion of Figure 3. The layered structure of $K_4Nb_6O_{17}$ is preserved within the scroll, as seen by the broad reflection at 5° and 040 reflection at about 11°. The peak at 28° has become the strongest reflection, since it is the 002 reflection from lattice planes contained within one sheet; *hkl* reflections with two or more nonzero indices have been extinguished by the exfoliation and scrolling process. The XRD patterns in the lower panel of Figure 3 show the thermal conversion of the scrolls to Nb_2O_5. The structural details of this transformation are discussed in more detail below.

Nitrogen adsorption isotherms of the scrolls and nanotubes were obtained to yield a Brunauer−Emmett−Teller (BET) surface area and pore size distribution according to the Barrett, Joyner, and Halenda (BJH) theory. The pore size distribution is shown in Figure 4, and a number of peaks are seen. We are not sure about the origins of the sharp peak at 2 nm for the scrolls, as the peak is greatly diminished when the adsorption data is modeled by an alternative theory such as density functional theory (DFT). The larger peak centered at 4 nm corresponds reasonably well with the inner radius measured from TEM images, which for the Nb_2O_5 nanotubes was 5.4 ± 1.0 nm (standard deviation, $n = 41$); hence, we ascribe this feature to the pores from the individual nanotubes. Larger pores of approximately 20 nm radius are also observed, perhaps because of the spaces between aggregates of tubes.

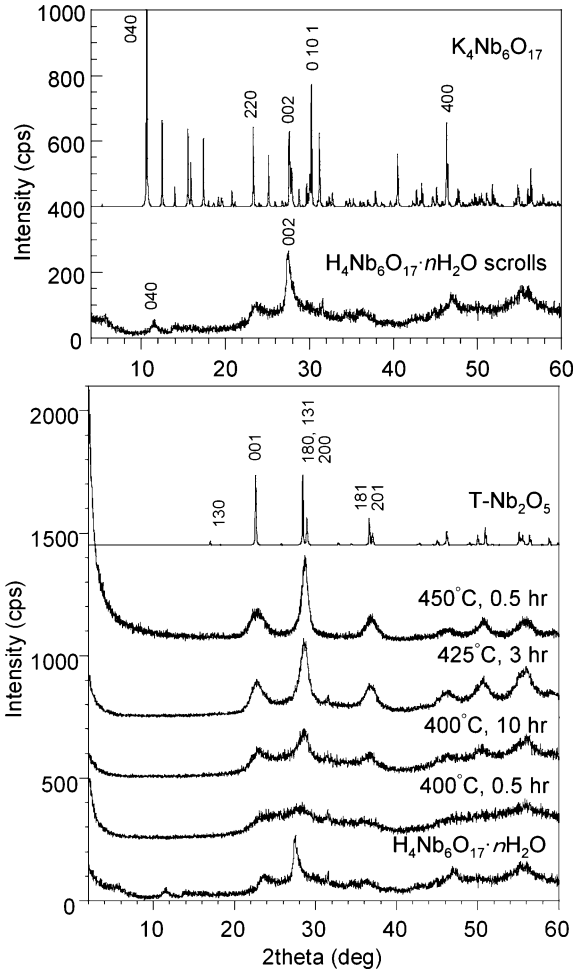

Figure 3. XRD patterns showing the transformation from $H_4Nb_6O_{17}{\cdot}nH_2O$ scrolls to Nb_2O_5.

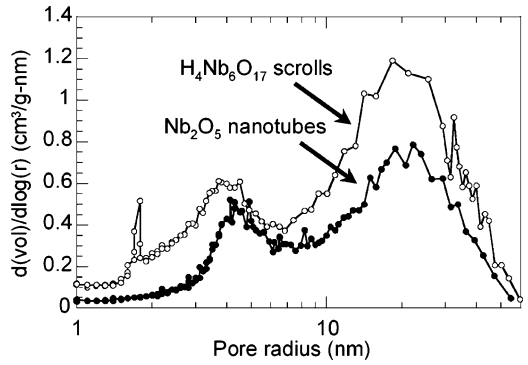

Figure 4. Pore size distribution of $H_4Nb_6O_{17}{\cdot}nH_2O$ scrolls and Nb_2O_5 nanotubes (nanotubes obtained after dehydration at 425 °C for 3 h).

The BET surface area was approximately 250−300 m^2/g, with some variation from batch to batch. In general, the specific surface area (S) of a tube can be calculated geometrically from the expression below:

$$S = \frac{(2\pi r_{OD} l) + (2\pi r_{ID} l)}{[(r_{OD}{}^2 - r_{ID}{}^2)\pi l]d} \quad (1)$$

where r_{ID} and r_{OD} are the inner and outer diameters of the

tube and d is the density of the material. This equation can be simplified and rearranged to yield the wall thickness (m), based on the surface area (m^2/g) and density (cm^3/g):

$$r_{OD} - r_{ID} = \frac{2 \times 10^{-6}}{Sd} \quad (2)$$

As mentioned above, depending on the batch, the surface area S of the tubes ranged between 250 m^2/g and 300 m^2/g. On the basis of the lattice parameters from XRD experiments, the density of $H_4Nb_6O_{17}\cdot 4.4H_2O$ is 3.91 g/cm^3, and that of anhydrous $H_4Nb_6O_{17}$ is approximately 3.6 g/cm^3. If one chooses a value of 275 m^2/g for the surface area and sets the density to 3.75 g/cm^3, then the calculated wall thickness is 1.9 nm, corresponding to a scroll that is wrapped around 2 to 3 times. This is slightly smaller than most wall thicknesses (ranging from 2−5 nm) observed in the TEM images.

Characterization of Nb_2O_5 Nanotubes. Because EDS spectra show that the scrolls do not contain potassium, we may write the following reaction for dehydrating the scrolls to convert them to Nb_2O_5 nanotubes:

$$H_4Nb_6O_{17}\cdot nH_2O \rightarrow 3Nb_2O_5 + (2 + n)H_2O \quad (3)$$

It is possible that some tetrabutylammonium cations remain in the scrolls. To ensure full exchange to the protonated form ($H_4Nb_6O_{17}$), after precipitation, the exfoliated scrolls were washed and stirred overnight in 0.5 M nitric or hydrochloric acid. Thermal gravimetric analysis (see Supporting Information**)** shows two weight losses between 230 and 450 °C, equivalent to a water loss of 1.9 mol, which is close to the 2 mol loss expected from eq 3. We can therefore conclude that little tetrabutylammonium remains in the scrolls after acid washing (also see Supporting Information for IR spectra, which shows only an extremely small C−H stretching peak). We also see a significant weight loss centered at 100 °C, which sets n in $H_4Nb_6O_{17}\cdot nH_2O$ at $n = 4.4$.

According to the thermal gravimetric results, dehydration is fairly complete at 425 °C. At this temperature, the tubes have not yet sintered, as can be seen in the TEM images of Figure 2b. The pore size distribution (Figure 4) is still centered on the same radius. The surface area of the tubes has decreased somewhat to 150−200 m^2/g. Most of this decrease is due to a change in the density of the material, rather than sintering. Upon formation of Nb_2O_5, the density of the material goes from approximately 3.75 g/cm^3 to 5.24 g/cm^3, resulting in a decrease in apparent surface area. Taking the surface area to be 175 m^2/g, the calculated tube wall thickness after dehydration is 2.2 nm, which again is slightly smaller than that observed by TEM; however, this is still consistent with the calculated wall thickness (1.9 nm) obtained before dehydration.

The series of XRD patterns in the lower panel of Figure 3 shows the scrolls as they are transformed into nanotubes at about 400 °C. Although many phases are known to exist for Nb_2O_5, a common progression found during the calcination of low-temperature precursors is

$$TT \rightarrow T \rightarrow B/M \rightarrow H \quad (4)$$

where the actual transition temperature is dependent on precursors, impurities, and so forth.[24] In terms of XRD, the TT and T phases are difficult to distinguish, and in fact, the T phase is thought to be simply a more ordered structure of the TT phase.[25−28] The structure of T−Nb_2O_5 is shown in Figure 1b. The xy plane is comprised of edge-shared NbO_6 and NbO_7 units. These are then linked by corner-sharing polyhedra along the z axis to form the three-dimensional structure. A small amount of additional Nb atoms (not shown) are scattered within the vacancies between the octahedral sites, in a loose sixfold coordination.[25,26]

Looking back at the edge-sharing network of purely octahedral units in $K_4Nb_6O_{17}$, it is clear that conversion to TT, T−Nb_2O_5 requires long-range diffusion of Nb and O atoms; in other words, the dehydration reaction cannot be topochemical. Hence, it would be difficult for a single-crystal nanotube to result. The electron diffraction pattern of an individual nanotube is shown in Figure 2b and shows evidence of multiple crystallites.

In order to determine crystallite sizes, the Scherrer equation was used to analyze the widths of the 28° (180, 131, 200) and 22° (001) diffraction peaks (Figure 3). For the sample heated to 400 °C, both peaks yielded crystallite sizes of approximately 4 to 5 nm, although it was hard to make an accurate determination because of excessive broadening in the lower angle peak and the contribution of two overlapping reflections to the higher angle peak. At 450 °C, the crystallite size L_{001} is approximately 4 nm, whereas $L_{180,131,200}$ is approximately 10 nm. This is noteworthy given that the tube wall thicknesses are on the order of 2 to 3 nm, smaller than the crystallite size determined from $L_{180,\ 131,\ 200}$. Although TEM images show that the tubes have started to sinter at 450 °C, there is a possibility that the anisotropy in crystallite size may be due to preferred orientation of the crystallites within the tube, with the 00l planes parallel to the tube walls.

The TEM image shown in Figure 5, combined with dark field imaging, supports this proposed texture. Figure 5a shows a single tube and its corresponding selected area electron diffraction (SAED) in the inset. In the SAED pattern, points A correspond to 001 type planes ($d = 3.93$ Å), whereas points B correspond to 180 type planes ($d = 3.14$ Å). Dark field imaging of the 001 spots (Figure 5b) illuminated the same areas as shown in the lattice fringe insets, where the fringes run parallel to the tube walls. This means that the lattice fringes are due to 001 reflections, and the planes run parallel to the tube walls. Another example is shown in the images in Figure 5d,e. In Figure 5e, crystallites with their 001 planes parallel to the electron beam have been illuminated. All of the illuminated crystallites are positioned on the wall areas of the tube, whereas in Figure 5f the crystallites with the 180 planes parallel to the beam are less localized on the walls of the tube. In either 001 dark field image, the entire walls are not illuminated since the

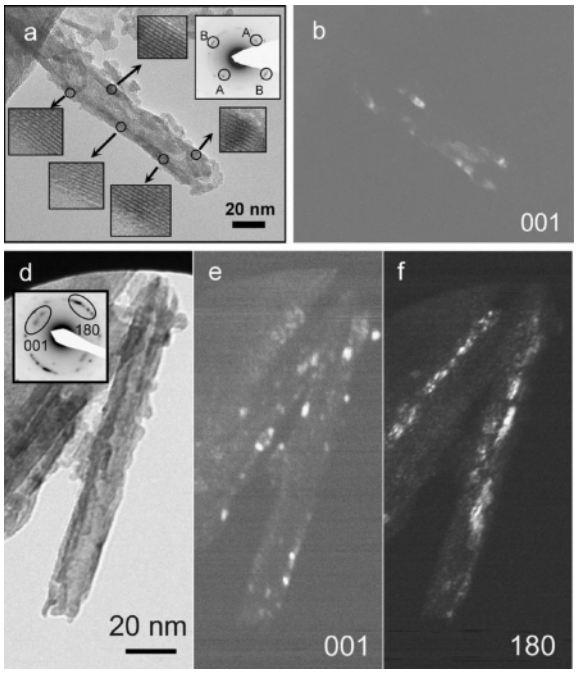

Figure 5. Bright field and dark field images of single Nb_2O_5 nanotubes.

tube walls are not thick or crystalline enough in all regions to provide enough diffraction contrast; close examination shows that the illuminated areas tend to be the thicker, darker sections of the tube walls in the bright field images. Nevertheless, the important point is that when the 001 crystallites are illuminated, they tend to localize on the tube walls, while the 180 crystallites do not; furthermore, the lattice fringes are parallel to the tube walls, which implies that there is a substantial degree of texturing with the 001 planes parallel to the tube walls.

Substituting tantalum for niobium had a somewhat surprising effect on the exfoliation behavior. Instead of forming scrolls, $TBA_xH_{1-x}Nb_3Ta_3O_{17}$ exfoliated to initially give predominantly large micrometer-sized sheets. Sonicating the suspensions with a probe consistently yielded a higher yield of Nb_3Ta_3 scrolls. Similar results were obtained with a Ta_6 sample, although in this case the scrolling yield depended on the batch. In general, complete conversion to scrolls was not observed in either case. Apparently, with Ta-substituted compounds, neither sonication nor sheet size affects the ability to scroll. Sheets caught in the act of scrolling can be seen (see Supporting Information). Unlike $K_4Nb_6O_{17}$, where a preferred scrolling direction has been reported, these semi-scrolled sheets seem to have no preferred scrolling direction. Some sheets were seen to be scrolling on all sides and with the two scrolling edges not at right angles to each other.

Is it possible that substitution with tantalum, whether it be partial or full, decreases the ability to scroll by alleviating the stress in the layers? Comparison by Rietveld refinement of the tantalates was difficult since both tantalates partially hydrate in atmosphere to form a less crystalline material. It is possible that stress is relieved by Ta substitution, because of its slightly larger size and greater tendency, relative to Nb, to adopt a regular octahedral coordination geometry.

In conclusion, $H_4Nb_6O_{17}$ scrolls were successfully dehydrated to form high surface area T−Nb_2O_5 polycrystalline nanotubes. This successful example of a thermal scroll-to-tube conversion shows that in many systems it may be possible to conduct the conversion without sintering and destroying the desired morphology. The next step is to scroll a layered precursor which may topochemically transform into a tube, potentially creating a single crystalline nanotube.

Acknowledgment. This work was supported by the National Science Foundation under Grant CHE-0616450.

Supporting Information Available: Experimental details, a figure comparing pore size distributions from BJH and NLDFT theories, an IR spectrum of $H_4Nb_6O_{17}\cdot nH_2O$ scrolls, and TEM images of tantalum-substituted scrolls. This material is available free of charge via the Internet at http://pubs.acs.org.

References

(1) Saupe, G. B.; Waraksa, C. C.; Kim, H.-N.; Han, Y. J.; Kaschak, D. M.; Skinner, D. M.; Mallouk, T. E. *Chem. Mater.* **2000**, *12*, 1556−1562.
(2) Du, G.; Chen, Q.; Yu, Y.; Zhang, S.; Zhou, W.; Peng, L.-M. *J. Mater. Chem.* **2004**, *14*, 1437−1442.
(3) Wörle, M.; Krumeich, F.; Bieri, F.; Muhr, H.-J.; Nesper, R. *Z. Anorg. Allg. Chem.* **2002**, *628*, 2778−2784.
(4) Muhr, H.-J.; Krumeich, F.; Schönholzer, U. P.; Bieri, F.; Niederberger, M.; Gauckler, L. J.; Nesper, R. *Adv. Mater.* **2000**, *12*, 231−234.
(5) Viculis, L. M.; Mack, J. J.; Kaner, R. B. *Science* **2003**, *299*, 1361.
(6) Li, Y. D.; Li, X. L.; He, R. R.; Zhu, J.; Deng, Z. X. *J. Am. Chem. Soc.* **2002**, *124*, 1411−1416.
(7) Mao, Y.; Wong, S. S. *J. Am. Chem. Soc.* **2006**, *128*, 8217−8226.
(8) Zhou, H.; Park, T.-J.; Wong, S. S. *J. Mater. Res.* **2006**, *21*, 2941−2947.
(9) Park, T.-J.; Mao, Y.; Wong, S. S. *Chem. Commun.* **2004**, 2708−2709.
(10) Mao, Y.; Kanungo, M.; Hemraj-Benny, T.; Wong, S. S. *J. Phys. Chem. B* **2006**, *110*, 702−710.
(11) Mao, Y.; Banerjee, S.; Wong, S. S. *Chem. Commun.* **2003**, 408−409.
(12) Seo, D.-S.; Lee, J.-K.; Kim, H. *J. Cryst. Growth* **2001**, *229*, 428−432.
(13) Wang, Y. Q.; Hu, G. Q.; Duan, X. F.; Sun, H. L.; Xue, Q. K. *Chem. Phys. Lett.* **2002**, *365*, 427−431.
(14) Zhang, S.; Peng, L.-M.; Chen, Q.; Du, G. H.; Dawson, G.; Zhou, W. Z. *Phys. Rev. Lett.* **2003**, *91*, 256103.
(15) Suzuki, Y.; Yoshikawa, S. *J. Mater. Res.* **2004**, *19*, 982−985.
(16) Wei, M.; Konishi, Y.; Zhou, H.; Sugihara, H.; Arakawa, H. *Solid State Commun.* **2005**, *133*, 493−497.
(17) Tsai, C. C.; Teng, H. *Chem. Mater.* **2006**, *18*, 367−373.
(18) Wang, N.; Lin, H.; Li, J.; Zhang, L.; Lin, C.; Li, X. *J. Am. Ceram. Soc.* **2006**, *89*, 3564−3566.
(19) Wang, X.; Li, Y. *Chem. Lett.* **2004**, *33*, 48−49.
(20) Schaak, R. E.; Mallouk, T. E. *Chem. Mater.* **2002**, *14*, 1455−1471.
(21) Ma, R.; Bando, Y.; Sasaki, T. *J. Phys. Chem. B* **2004**, *108*, 2115−2119.
(22) Gasperin, M.; Le Bihan, M.-T. *J. Solid State Chem.* **1982**, *43*, 346−353.
(23) Du, G. H.; Peng, L.-M.; Chen, Q.; Zhang, S.; Zhou, W. Z. *Appl. Phys. Lett.* **2003**, *83*, 1638−1640.
(24) Schafer, H.; Gruehn, R.; Schulte, F. *Angew. Chem., Int. Ed.* **1966**, *5*, 40−52.
(25) Kato, K.; Tamura, S. *Acta Crystallogr., Sect. B Struct. Sci.* **1975**, *B31*, 673−677.
(26) Tamura, S.; Kato, K.; Goto, M. *Z. Anorg. Allg. Chem.* **1974**, *410*, 313−315.
(27) Weissman, J. G.; Ko, E. I.; Wynblatt, P.; Howe, J. M. *Chem. Mater.* **1989**, *1*, 187−193.
(28) Gatehouse, B. M.; Wadsley, A. D. *Acta. Crystallogr.* **1964**, *17*, 1545−1554.

NL0708260